

# Class V $\beta$ -tubulin alters dynamic instability and stimulates microtubule detachment from centrosomes

Rajat Bhattacharya, Hailing Yang, and Fernando Cabral

Department of Integrative Biology and Pharmacology, University of Texas Medical School, Houston, TX 77030

**ABSTRACT** A multigene family produces tubulin isotypes that are expressed in a tissue-specific manner, but the role of these isotypes in microtubule assembly and function is unclear. Recently we showed that overexpression or depletion of  $\beta 5$ -tubulin, a minor isotype with wide tissue distribution, inhibits cell division. We now report that elevated  $\beta 5$ -tubulin causes uninterrupted episodes of microtubule shortening and increased shortening rates. Conversely, depletion of  $\beta 5$ -tubulin reduces shortening rates and causes very short excursions of growth and shortening. A tubulin conformation-sensitive antibody indicated that the uninterrupted shortening can be explained by a relative absence of stabilized patches along the microtubules that contain tubulin in an assembly-competent conformation and normally act to restore microtubule growth. In addition to these changes in dynamic instability, overexpression of  $\beta 5$ -tubulin causes fragmentation that results from microtubule detachment from centrosomes, and it is this activity that best explains the effects of  $\beta 5$  on cell division. Paclitaxel inhibits microtubule detachment, increases the number of assembly-competent tubulin patches, and inhibits microtubule shortening, thus providing an explanation for why the drug can counteract the phenotypic effects of  $\beta 5$  overexpression. On the basis of these observations, we propose that cells can use  $\beta 5$ -tubulin expression to adjust the behavior of the microtubule cytoskeleton.

## Monitoring Editor

Stephen J. Doxsey  
University of Massachusetts

Received: Oct 13, 2010

Revised: Dec 2, 2010

Accepted: Jan 21, 2011

## INTRODUCTION

Microtubules are essential cytoskeletal organelles involved in vesicle transport, cell motility, chromosome segregation, and cell division. They are composed of  $\alpha\beta$ -tubulin heterodimers that assemble into linear protofilaments that associate laterally to form hollow tubes ~25 nm in diameter. Vertebrate genomes have been shown to encode six to seven isotypes of both  $\alpha$ - and  $\beta$ -tubulin, some of which are expressed ubiquitously, whereas others are expressed in a tissue-specific manner (Ludueno, 1998; Sullivan, 1988). The  $\alpha$ -tubulin proteins are highly conserved and differ by only a few residues; but the  $\beta$ -tubulins differ significantly in their C-terminal fifteen residues

and, to a lesser extent, in other regions of the protein as well. Based on their C-terminal sequences,  $\beta$ -tubulin isotypes can be assigned to seven distinct classes named  $\beta 1$ ,  $\beta 2$ ,  $\beta 3$ ,  $\beta 4a$ ,  $\beta 4b$ ,  $\beta 5$ , and  $\beta 6$  (Lopata and Cleveland, 1987). Most cells express a subset of these isotypes, but it is unclear whether the different isotypes are functionally interchangeable or whether they impart unique properties onto the microtubules into which they assemble. One hypothesis, originally formulated by Fulton and Simpson (1976), posits that different tubulin isotypes subserve different functions. However, immunostaining studies using isotype-specific antibodies indicated that interphase, spindle, and flagellar microtubules incorporated all of the isotypes that were present in the cell (Lewis *et al.*, 1987; Lopata and Cleveland, 1987; Sawada and Cabral, 1989). Thus there was no functional segregation of isotypes into discreet subcellular structures. Additional studies indicated that this also held true for transfected isotypes that were not normally produced by the cell (Bond *et al.*, 1986; Joshi *et al.*, 1987; Lewis *et al.*, 1987). It would thus appear that tubulin isotypes are used interchangeably to form cellular microtubules, but these studies left open the possibility that incorporating different isotypes might alter the properties of the microtubules.

This article was published online ahead of print in MBoC in Press (<http://www.molbiolcell.org/cgi/doi/10.1091/mbc.E10-10-0822>) on February 2, 2011.

Address correspondence to: Fernando Cabral ([fernando.r.cabral@uth.tmc.edu](mailto:fernando.r.cabral@uth.tmc.edu)).

Abbreviations used: ptx, paclitaxel.

© 2011 Bhattacharya *et al.* This article is distributed by The American Society for Cell Biology under license from the author(s). Two months after publication it is available to the public under an Attribution-Noncommercial-Share Alike 3.0 Unported Creative Commons License (<http://creativecommons.org/licenses/by-nc-sa/3.0>).

"ASCB<sup>®</sup>," "The American Society for Cell Biology<sup>®</sup>," and "Molecular Biology of the Cell<sup>®</sup>" are registered trademarks of The American Society of Cell Biology.

In vitro studies using purified  $\beta$ -tubulin isoforms indicated the existence of differences in drug binding and assembly (Banerjee and Luduena, 1992; Lu and Luduena, 1994; Panda *et al.*, 1994), but the question of whether similar changes can be seen in living cells has been more difficult to address. In *Aspergillus nidulans*, a  $\beta$ -tubulin specifically expressed during conidiation was able to substitute for the isoform normally used during hyphal growth (May, 1989). Similarly, in transgenic mice, there were no effects on cardiac function when the predominant  $\beta$ 4b isoform was replaced with  $\beta$ 1 (Takahashi *et al.*, 2003). On the other hand, other genetic studies support the notion of functional discrimination among tubulin isoforms. For example, studies in *Drosophila* indicated the presence of a specific germ line tubulin isoform required for the assembly of sperm flagella axonemes (Hoyle and Raff, 1990). Specific tubulin isoforms have also been reported to be necessary for the formation of the 15 protofilament microtubules in touch receptor cells of *Caenorhabditis elegans* (Savage *et al.*, 1989). In mammals, functional specificity of tubulin isoforms has been found in mice where it was reported that knocking out the hematopoietic  $\beta$ 6-tubulin isoform led to altered platelet morphology and clotting times (Schwer *et al.*, 2001). The picture that emerges from these studies is that different tubulins are all able to coassemble, and in doing so they may, or may not, alter the properties and functions of the microtubules that they form.

Recently we set out to resolve functional differences among  $\beta$ -tubulins by transfecting CHO cells to express each mammalian isoform under the control of a tetracycline-regulated promoter and then testing the cells for effects on growth, microtubule assembly, and drug sensitivity. Using this approach, we found that overexpressing  $\beta$ 5-tubulin, a minor ubiquitously expressed isoform, resulted in disruption of the microtubule cytoskeleton, defects in cell division, and resistance to paclitaxel, a drug that is known to promote microtubule assembly (Bhattacharya and Cabral, 2004). Moreover, cells with high  $\beta$ 5 expression were not only resistant to the drug, but they required its presence for cell division. Surprisingly, when cells were depleted of  $\beta$ 5, they again experienced problems in mitosis, indicating that this isoform is needed in small amounts for cell division (Bhattacharya *et al.*, 2008). In an effort to understand how increasing or depleting  $\beta$ 5 is able to interfere with microtubule function, we used live cell imaging to examine the effects of  $\beta$ 5 overexpression or depletion on microtubule behavior. We report that  $\beta$ 5 increases the rate and extent of microtubule shortening and that this action is reversed by the presence of paclitaxel. The extended shortening phases caused by  $\beta$ 5 incorporation appear to be mediated by a large reduction in the number of stabilized microtubule patches called "GTP remnants" that normally interrupt the process of depolymerization. In addition, excessive  $\beta$ 5 incorporation causes the production of microtubule fragments that are generated by

enhanced detachment of microtubules from centrosomes. This latter activity is also reversed by paclitaxel and appears to best explain the reduced microtubule content and problems in cell division exhibited by  $\beta$ 5 overexpressing cells.

## RESULTS

### HA $\beta$ 5-tubulin incorporation alters microtubule stability

Immunofluorescence was used to examine microtubule organization in cells that overexpressed or were depleted of  $\beta$ 5-tubulin. HA $\beta$ 5c8, a cell line in which transfected HA $\beta$ 5-tubulin makes up ~50% of the total tubulin content (Bhattacharya and Cabral, 2004), exhibited a highly disrupted microtubule cytoskeleton that contained numerous short (arrowheads, Figure 1A) and long (arrows, Figure 1A) microtubule fragments. In addition, the cells were larger than normal and had enlarged and/or fragmented nuclei, features that are typical of cells that have failed to properly segregate chromosomes or undergo cell division (Abraham *et al.*, 1983; Cabral and Barlow, 1991; Kung *et al.*, 1990). CHO cells expressing short hairpin RNA (shRNA) to reduce the endogenous  $\beta$ 5-tubulin, on the other hand, had abundant normal-looking microtubules but again experienced mitotic defects as indicated by their large size and abnormal nuclei (Figure 1B). The results indicated that excessive incorporation of  $\beta$ 5 caused disruption of the cellular microtubules and led to

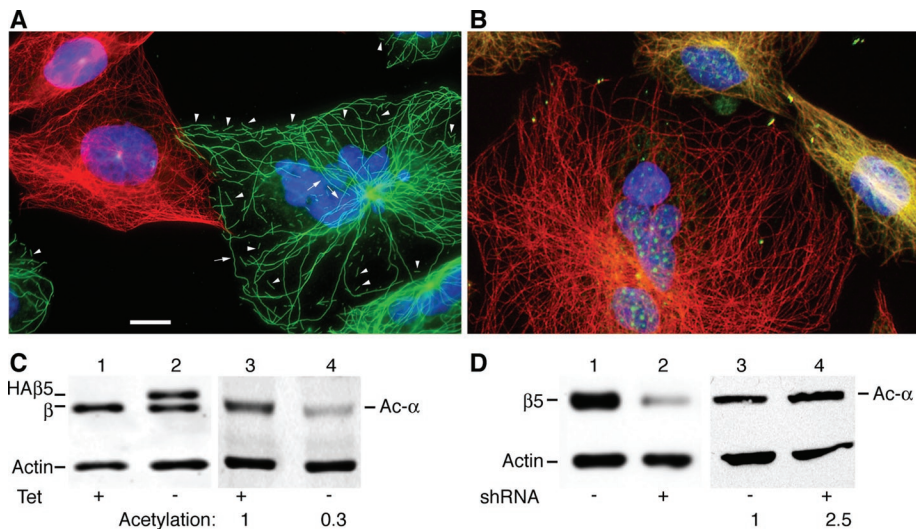


**FIGURE 1:** Changes in  $\beta$ 5-tubulin expression alter microtubule stability and inhibit cell division. (A) HA $\beta$ 5c8 cells (green) were grown 2 d without tetracycline to allow HA $\beta$ 5-tubulin overexpression and were subsequently fixed and stained with DAPI to label the DNA (blue) as well as antibodies to the HA tag (green) and to endogenous  $\alpha$ -tubulin (red). Untransfected CHO cells (red) were coplated as a control. Note that the HA $\beta$ 5-tubulin-overexpressing cells appear green because the HA tag antibody interferes with the binding of the  $\alpha$ -tubulin antibody. Some of the abundant long (arrows) and short (arrowheads) microtubule fragments found in the transfected cells are indicated. (B) CHO cells were transfected with  $\beta$ 5-specific shRNA and allowed to grow for 4 d to deplete the endogenous protein. The fixed cells were stained with DAPI (blue),  $\beta$ 5-specific antibody (green), and  $\alpha$ -tubulin antibody (red). The  $\beta$ 5-depleted cells appear red as they only stain with the  $\alpha$ -tubulin antibody. Untransfected cells expressing  $\beta$ 5 appear as yellow or orange. (C) HA $\beta$ 5c8 cells were grown with (lanes 1 and 3) or without (lanes 2 and 4) tetracycline to induce HA $\beta$ 5-tubulin expression. Proteins were separated on SDS gels, and the Western blots were stained with antibody 18D6 that recognizes all isoforms of  $\beta$ -tubulin (lanes 1 and 2) or antibody 611B1 specific for acetylated  $\alpha$ -tubulin (lanes 3 and 4). (D) CHO cells transfected with empty vector (lanes 1 and 3) or  $\beta$ 5 shRNA (lanes 2 and 4) were grown 7 d in hygromycin to remove untransfected cells, and the Western blots were stained with antibodies specific for  $\beta$ 5-tubulin (lanes 1 and 2) or acetylated  $\alpha$ -tubulin (lanes 3 and 4). An antibody to actin was included to act as a gel-loading control in (C) and (D). Bands were quantified by fluorescence emission as described in *Materials and Methods*, and the relative levels of  $\alpha$ -tubulin acetylation (Ac- $\alpha$  divided by actin and normalized to the value for lane 3 set at 1) are indicated below lanes 3 and 4 in (C) and (D). Scale bar, 10  $\mu$ m.

decreased levels of polymerized tubulin but that some low level of  $\beta 5$ -tubulin was necessary for normal microtubule function during mitosis.

To more quantitatively determine the relative stability of the microtubules in these cells, we measured the amount of acetylated tubulin in cell lysates. Acetylation is a posttranslational modification of  $\alpha$ -tubulin that occurs preferentially on microtubules rather than soluble tubulin (Maruta *et al.*, 1986). The modification increases with time and thereby acts as a measure of a microtubule's age before it undergoes depolymerization. HA $\beta 5$ c8, which expresses HA $\beta 5$ -tubulin in the absence but not in the presence of tetracycline (Figure 1C, lanes 1 and 2), exhibited a threefold reduction in acetylated  $\alpha$ -tubulin when the cells were grown overnight without tetracycline (Figure 1C, lanes 3 and 4). Because there were very few microtubules in HA $\beta 5$ -overexpressing cells and because only polymerized tubulin is acetylated, we also compared the relative amount of acetylated tubulin in microtubule preparations instead of whole cell lysates and again found a threefold reduction in HA $\beta 5$ -overexpressing cells (data not shown). In contrast to the results obtained with  $\beta 5$  overexpression, CHO cells that were transfected with shRNA had an 80–90% reduction in endogenous  $\beta 5$  compared with vector-transfected control cells (Figure 1D, lanes 1 and 2), and the level of acetylated  $\alpha$ -tubulin increased ~2.5-fold as a result of the  $\beta 5$  depletion (Figure 1D, lanes 3 and 4). This value is consistent with immunofluorescence experiments that also indicate increased tubulin acetylation when  $\beta 5$  is depleted (Bhattacharya *et al.*, 2008). We concluded from these experiments that the longevity of microtubules is significantly affected by the level of  $\beta 5$ -tubulin.

### HA $\beta 5$ -tubulin overexpression does not alter microtubule nucleation

In an effort to explain the reduced number of microtubules in HA $\beta 5$ -overexpressing cells, we tested the possibility that microtubule nucleation might be affected. A 50:50 mixture of wild-type and HA $\beta 5$ -overexpressing cells was plated and treated with 150 ng/ml colcemid for 2 h to disrupt the existing microtubule network; microtubule regrowth was then monitored by fixing the cells and staining them with anti-tubulin and anti-HA antibodies at various times after washing out the drug. We found that wild-type and HA $\beta 5$ -expressing cells exhibited a similar time course for microtubule regrowth (Supplemental Figure S1A). In both cases, there was an initial lag of ~10 min before readily visible microtubule growth was apparent, and return of the microtubule cytoskeleton required ~30 min.

We also tested the effect of reducing  $\beta 5$  on microtubule nucleation. To deplete endogenous  $\beta 5$ , CHO cells were transfected with a pmCherryH2B-c $\beta 5$  plasmid (see *Materials and Methods*) that expresses both mCherry-H2B, to act as a marker for transfected cells, and the shRNA that targets CHO  $\beta 5$ -tubulin. We knew from past experience that tubulin is a very stable protein and that cells require considerable time before they are depleted of  $\beta 5$  and begin to stop dividing (Bhattacharya *et al.*, 2008). We therefore performed measurements 4 d after transfection and identified  $\beta 5$ -depleted cells as those that were larger than normal and had large red nuclei. The time course for renucleation of microtubules in

$\beta 5$ -depleted cells also appeared to be normal (Supplemental Figure S1B).

The experiments depicted in Supplemental Figure S1 monitored microtubule formation under conditions in which the cells were first perturbed to depolymerize existing microtubules, thereby increasing the free tubulin content that could drive microtubule regrowth and potentially mask  $\beta 5$ -tubulin effects. To assess whether there are differences in nucleation under nonperturbed steady-state conditions, cells were transfected with a plasmid encoding EB1-GFP, a protein that binds to the tips of growing microtubules (Akhmanova and Steinmetz, 2008). The cells were then viewed by time-lapse fluorescence microscopy and the numbers of EB1 "comets" emerging from the centrosomes were counted in control, HA $\beta 5$ -overexpressing, and  $\beta 5$ -depleted cells (Figure 2). Again, there were no significant differences among the three cell types. We thus conclude that the incorporation of  $\beta 5$  into microtubules does not significantly affect their nucleation rates.

### Microtubule shortening is stimulated by HA $\beta 5$ -tubulin overexpression

Because microtubule nucleation appeared to be unaffected by  $\beta 5$ -tubulin, we turned our attention to the effects of this isotype on microtubule dynamics. Microtubule plus ends grow out from the centrosome toward the plasma membrane and are known to transition between periods of growth and shortening interspersed with periods of pause in which there is no change in length, a behavior called dynamic instability (Mitchison and Kirschner, 1984). According to the currently accepted model for this behavior, a microtubule can elongate as long as GTP is bound to  $\beta$ -tubulin at the plus end to form a "GTP cap." Hydrolysis of the GTP to GDP causes a conformational change that results in microtubule "catastrophe," that is, a transition from growth or pause to a shortening phase. Reestablishment of the GTP cap results in "rescue," a transition from shortening to a pause or growth phase. Thus microtubules at steady state exhibit stochastic episodes of growth and shortening that can be defined by a series of measurable parameters (Jordan and Wilson, 1998). To test the effect of  $\beta 5$  expression on these parameters, we transfected cells with EGFP-MAP4 to fluorescently label the microtubules (Olson *et al.*, 1995) and directly observed changes in microtubule length by time-lapse

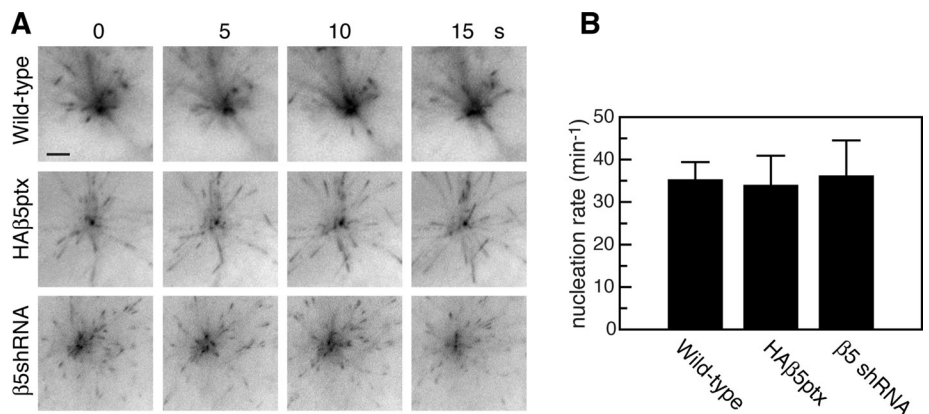


**FIGURE 2:**  $\beta 5$ -Tubulin does not affect microtubule nucleation. Cells were transfected with EB1-GFP, and live cell images were captured at 5-s intervals. (A) Four consecutive images around the centrosome are shown for wild-type CHO cells, HA $\beta 5$ ptx cells deprived of paclitaxel 16 h, and wild-type CHO cells 4 d after transfection with  $\beta 5$ shRNA. The images were inverted to improve contrast. (B) Relative nucleation rates were quantified by drawing two concentric rings (3.5 and 7.5  $\mu$ m diameter) around the centrosome in a series of images and counting the number of EB1 comets passing through the annulus per cell per min. Scale bar, 2  $\mu$ m.

microscopy. Previous studies have shown that overexpression or depletion of MAP4 has no observable effect on microtubule assembly, paclitaxel resistance, or cell survival (Barlow *et al.*, 1994; Wang *et al.*, 1996). More recently we showed that microtubule dynamics measured using EGFP-MAP4 agrees with data obtained using fluorescent tubulin microinjection in wild-type CHO cells (Kamath *et al.*, 2005; Ganguly *et al.*, 2010; Yang *et al.*, 2010). Thus it is unlikely that EGFP-MAP4 significantly alters microtubule dynamics in transfected cells.

As we previously reported, cells that express high levels of HA $\beta$ 5 are paclitaxel-dependent (Bhattacharya and Cabral, 2004). For measuring microtubule dynamics, we therefore used HA $\beta$ 5c8 cells that were maintained in paclitaxel (HA $\beta$ 5ptx). These cells, like HA $\beta$ 5c8, contain ~50% of their total  $\beta$ -tubulin as HA $\beta$ 5. HA $\beta$ 5ptx grows normally and has a normal microtubule cytoskeleton in the presence of 100 nM paclitaxel; but when maintained at lower drug concentrations, the cells cease to divide and exhibit a disrupted microtubule cytoskeleton similar to HA $\beta$ 5c8 cells (Supplemental Figure S2). The advantage of using HA $\beta$ 5ptx is that the effects of HA $\beta$ 5 overexpression can be assessed rapidly by paclitaxel removal, whereas HA $\beta$ 5c8 requires more than 24 h of induction before HA $\beta$ 5-tubulin reaches steady-state levels.

Life history plots showing time-dependent changes in microtubule length for wild-type and HA $\beta$ 5ptx cells incubated with and without paclitaxel are shown in Figure 3, A–D. Wild-type microtubules exhibited dynamic instability behavior characterized by frequent excursions of growth and shortening (Figure 3A). As previously reported by us and others (Jordan *et al.*, 1993; Ganguly *et al.*, 2010), addition of paclitaxel suppressed the dynamic instability be-

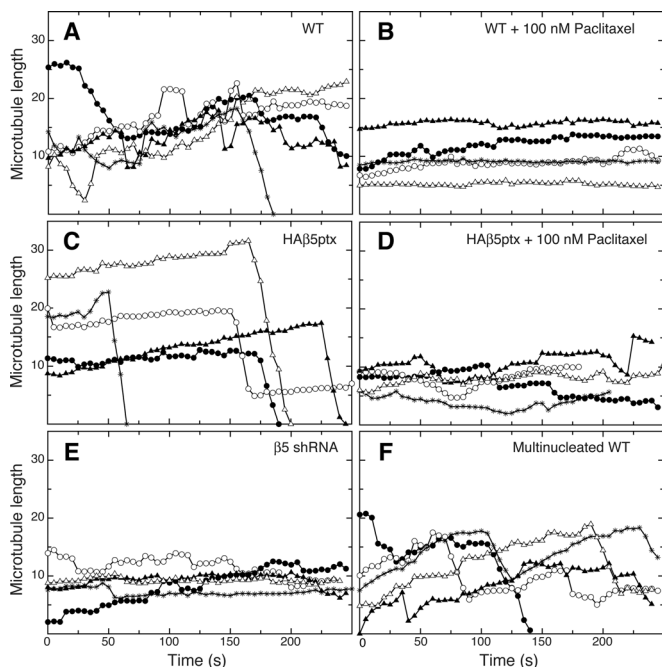


**FIGURE 3:** Microtubule life history plots. Wild-type CHO cells (A), HA $\beta$ 5ptx cells deprived of paclitaxel 16 h (C), and WT cells 4 d after transfection with  $\beta$ 5shRNA (E) were transfected with EGFP-MAP4 and viewed by time-lapse fluorescence microscopy. Microtubule lengths were measured from an arbitrary reference point in successive images taken 5 s apart and plotted vs. time. Each line represents a separate microtubule. Measurements were also carried out on wild-type and HA $\beta$ 5ptx cell lines treated with 100 nM paclitaxel (B and D) and on the small fraction (<5%) of large multinucleated cells that are typically found in wild-type CHO cell populations (F).

havior (Figure 3B). Unexpectedly, overexpression of HA $\beta$ 5-tubulin also suppressed overall dynamic instability; but following these variable periods of relatively static behavior, many of the microtubules were seen to undergo sudden rapid and largely uninterrupted shortening events that frequently led to their complete depolymerization (Figure 3C). During the 5-min periods that the cells were under observation, ~60–70% of the cellular microtubules were seen to undergo these long uninterrupted depolymerization phases. Addition of paclitaxel to HA $\beta$ 5ptx cells at a concentration that allowed normal cell division did not restore microtubule dynamics to a “wild-type” condition; rather, the dynamics remained relatively static, but the long uninterrupted shortening events no longer occurred (Figure 3D).

The parameters that describe dynamic instability were consistent with these gross observations (Supplemental Table S1). Because cells that overexpress or are depleted of  $\beta$ 5 become large and multinucleated, we had concerns that wild-type cells might not provide the best control for comparisons. We therefore also measured dynamic instability in the small percentage of large multinucleated cells that occur naturally in CHO cultures despite their having normal  $\beta$ 5-tubulin immunofluorescence. The results showed that microtubules in these cells behaved similarly to microtubules in diploid wild-type CHO cells except for small possible decreases in the growth and shortening rates (Figure 3F and Supplemental Table S1). We show a graphic comparison of the critical parameters that describe microtubule dynamic instability for HA $\beta$ 5ptx and multinucleated cells in Figure 4. Consistent with the time-lapse observations, microtubules in the HA $\beta$ 5-expressing cells had a lower frequency of catastrophe and rescue, and they spent more time in a paused state, leading to an overall lower dynamicity. The microtubules exhibited a near normal rate of growth; but significantly, they had an approximately twofold increase in their rate of shortening. To be certain that these changes were not restricted to the HA $\beta$ 5ptx cells, we collected more limited data using HA $\beta$ 5c8 by removing tetracycline for 2 d and obtained very similar results (data not shown).

Addition of paclitaxel to the HA $\beta$ 5-overexpressing cells potentially reversed the parameters (shortening rate, catastrophe frequency,

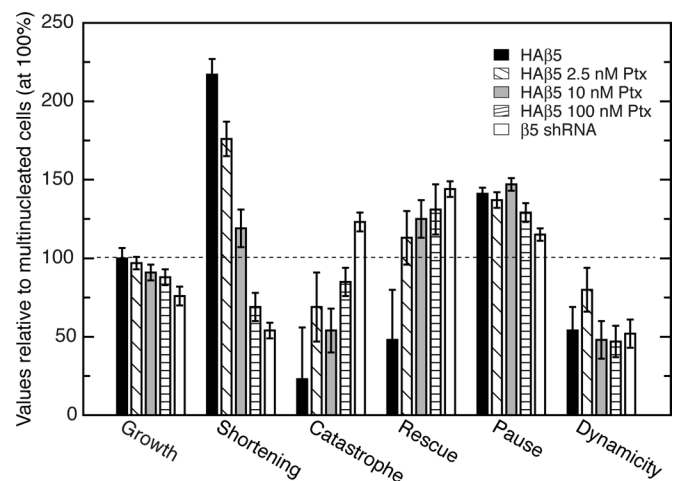


**FIGURE 4:** Effects of  $\beta$ 5-tubulin on microtubule dynamics. Values describing several of the parameters of dynamic instability are plotted relative to multinucleated cells in a wild-type CHO population set at 100% (dotted horizontal line). HA $\beta$ 5-overexpressing cells grown with increasing concentrations of paclitaxel (Ptx) and wild-type CHO cells depleted of  $\beta$ 5 ( $\beta$ 5 shRNA) are compared. The full set of numbers can be found in Supplemental Table S1.

and rescue frequency) that were most affected by HA $\beta$ 5 overexpression, but had only modest effects on the other parameters (Supplemental Table S1 and Figure 4). The high rate of microtubule shortening, the high frequency of long uninterrupted shortening events, and the ability of paclitaxel to reverse these consequences of HA $\beta$ 5 overexpression would seem to argue that these changes in microtubule behavior are responsible for the low amount of polymerized tubulin in HA $\beta$ 5-overexpressing cells. However, it should be noted that paclitaxel concentrations as low as 10 nM were able to substantially reduce the shortening rate (Figure 4) and the frequency of long uninterrupted shortening events (Supplemental Table S1), yet were not able to rescue cell division or normalize polymerized tubulin levels in HA $\beta$ 5ptx (Supplemental Figure S2). We therefore conclude that changes in dynamic instability may contribute to the phenotype of HA $\beta$ 5-overexpressing cells, but they are not sufficient.

### Depletion of $\beta$ 5-tubulin suppresses microtubule dynamics

If the increased shortening rate and lower frequencies of catastrophe and rescue seen in HA $\beta$ 5ptx microtubules were due to the overexpression of  $\beta$ 5-tubulin, we predicted that depletion of  $\beta$ 5 in wild-type cells should cause the opposite effects. To deplete  $\beta$ 5-tubulin, CHO cells were transfected with pmCherry-c $\beta$ 5 shRNA, they were transfected again at day 2 with EGFP-MAP4, and microtubule movements were recorded by time-lapse microscopy at day 4. Transfected cells were identified by their red nuclei created by the expression of the mCherry-H2B gene in the plasmid. In addition, transfected cells with low  $\beta$ 5 expression were larger than normal and had a larger nuclear size because  $\beta$ 5 depletion interferes with cell division (Bhattacharya *et al.*, 2008). Life history plots showed that microtubules in  $\beta$ 5-depleted cells also had significantly suppressed microtubule dynamics (Figure 3E). Unlike HA $\beta$ 5ptx cells, however, microtubule shortening rates were about twofold lower than normal, whereas catastrophe and rescue frequencies were somewhat elevated (Supplemental Table S1 and Figure 4). These effects are just the opposite of those seen with HA $\beta$ 5 overexpression and therefore strengthen the argument that the changes we measured in microtubule dynamic instability behavior are specifically caused by the modulation of  $\beta$ 5 content. The more than fourfold difference in the microtubule shortening rate between HA $\beta$ 5-overexpressing cells and  $\beta$ 5-depleted cells indicates that this is the parameter that is most sensitive to changes in  $\beta$ 5 content. In addition, long uninterrupted shortening phases, which occurred at high frequency in HA $\beta$ 5-overexpressing cells and were occasionally observed in wild-type cells, were exceedingly rare in  $\beta$ 5-depleted cells (Supplemental Table S1).

One curious finding was the observation that the overall microtubule dynamics appeared to be suppressed both in  $\beta$ 5-overexpressing cells that had few microtubules and in  $\beta$ 5-depleted cells that had abundant stable microtubules. We do not currently understand the basis for this phenomenon, but we note that drugs able to promote or inhibit microtubule assembly also suppress microtubule dynamics by an

unknown mechanism (Jordan and Wilson, 2004). Taken together, the results suggest that dynamic instability is not the main driver for microtubule assembly; rather, it may act only as a modulator of microtubule behavior.

### $\beta$ 5-Tubulin reduces the abundance of GTP remnants in microtubules

Microtubules elongate by the addition of  $\alpha\beta$ -tubulin heterodimers that contain GTP on both subunits. As the microtubules form, slow hydrolysis of GTP on the  $\beta$ -subunit is stimulated, causing most of the assembled tubulin to be in a GDP-bound state but leaving a cap of GTP-bound  $\beta$ -subunits at the growing tip of the microtubule (Mitchison and Kirschner, 1987). Recently an antibody was described that specifically recognizes the GTP-bound conformation of tubulin. The antibody was shown to stain growing microtubule ends where the GTP cap is expected to reside; but, surprisingly, additional patches representing "GTP remnants" were also found along the microtubule surface (Dimitrov *et al.*, 2008). The authors suggested that these GTP remnants might be responsible for the rescue events that stop depolymerization and allow microtubules to resume growth. To test whether  $\beta$ 5 incorporation affected these GTP remnants, we stained HA $\beta$ 5-overexpressing and  $\beta$ 5-depleted cells with the antibody. As shown in Figure 5A, wild-type CHO microtubules had occasional staining representing GTP remnants (red fluorescence) along their surface. In contrast, the microtubules in HA $\beta$ 5-overexpressing cells grown without paclitaxel were almost devoid of GTP remnants, an observation that may explain why these microtubules exhibited long uninterrupted depolymerization phases in live cell imaging experiments (see Figure 3). Consistent with this interpretation, treating these cells with paclitaxel or depleting  $\beta$ 5 from wild-type cells, treatments that essentially eliminate long depolymerization events, greatly increased the number of GTP remnants (Figure 5, A and B). It thus appears that  $\beta$ 5-tubulin plays a significant role in determining the existence of GTP remnants.

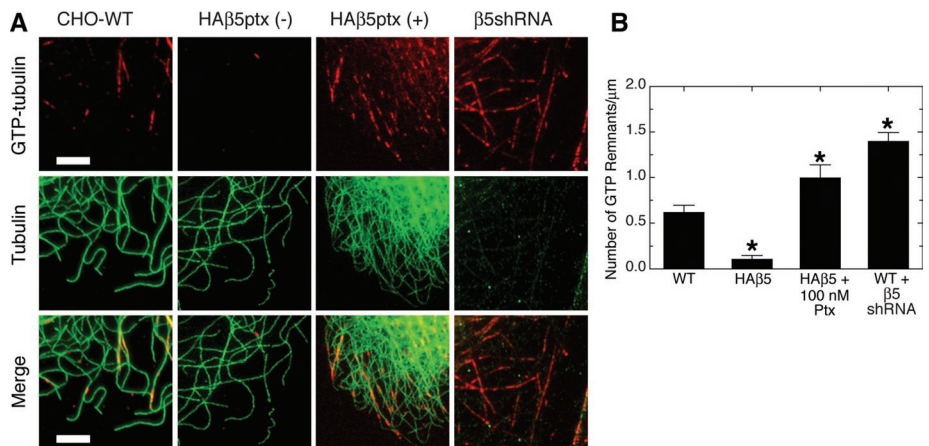


**FIGURE 5:**  $\beta$ 5-Tubulin affects the number of GTP remnants. (A) Untransfected wild-type CHO cells, HA $\beta$ 5ptx cells grown 2 d without paclitaxel (-), HA $\beta$ 5ptx cells maintained in 100 nM paclitaxel (+), and CHO cells 4 d after transfection with shRNA to deplete  $\beta$ 5 were permeabilized and stained with antibody hMB11 that recognizes the GTP-bound conformation of  $\beta$ -tubulin (red). The cells were then fixed in methanol and stained with antibodies to  $\alpha$ -tubulin (green) except for the  $\beta$ 5shRNA cells, which were treated instead with an antibody specific for  $\beta$ 5-tubulin (also green). The absence of green microtubules in these latter cells indicates that they are depleted of  $\beta$ 5. Other, presumably nontransfected, cells in the population stained positively for  $\beta$ 5 (not shown). Bar, 5  $\mu$ m. (B) For each of the indicated cells and treatments, the number of GTP remnants were counted and divided by the microtubule length. A total of 30 peripheral microtubules in five separate cells were measured for each experiment. The values represent the mean  $\pm$  SEM; \*,  $P < 0.01$ .

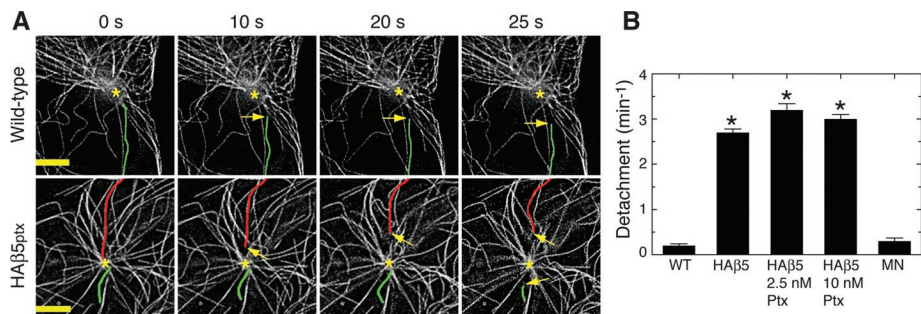


**FIGURE 6:** Microtubule detachment from centrosomes. (A) Wild-type and HAβ5ptx cells were transfected with EGFP-MAP4 and grown without paclitaxel for 16 h. Live cell images were obtained at 5-s intervals using a 100× objective and then deconvolved to enhance contrast. The relative times of the clips in the time-lapse sequence are shown. Asterisks mark the position of the centrosome. Microtubules detaching from the centrosome are shown in red and green. Arrows point to the minus ends of microtubules that detached during the 25-s sequence. (B) The number of detachments per minute was calculated by observing five to six cells for 5 min each. HAβ5ptx cells (HAβ5) were also treated with 100 nM paclitaxel (Ptx), but no detachments were seen under those conditions. Similarly, no detachments were seen in wild-type cells (WT) depleted of β5. Note that naturally occurring multinucleated cells (MN) had a similar rate of microtubule detachment as wild-type cells. The values represent the mean ± SD; \*,  $P < 0.01$ . Scale bars, 5 μm.

### HAβ5 overexpression induces microtubule detachment from centrosomes

Although we found that the β5-tubulin content played a very significant role in determining the dynamic behavior of microtubules, the changes that we measured appeared to be insufficient to explain the highly disrupted microtubule cytoskeleton of cells that overexpress HAβ5. This conclusion is most strikingly supported by the observation that 10 nM paclitaxel, a concentration that reversed the elevated shortening rate and the frequent uninterrupted depolymerization phases exhibited by microtubules in HAβ5-overexpressing cells, was insufficient to restore a normal level of microtubule polymer, prevent the formation of microtubule fragments, or allow the cells to divide (Supplemental Figure S2). In other recent studies, we found that some tubulin mutations produce a disrupted microtubule cytoskeleton similar to that seen in HAβ5-overexpressing cells, and showed that the microtubule fragments formed because of an increased frequency of microtubule detachment from centrosomes (Ganguly *et al.*, 2010). To determine whether overexpression of HAβ5-tubulin disrupts microtubules by a related mechanism, we carried out time-lapse microscopic studies in the centrosomal area of wild-type and HAβ5ptx cells incubated without paclitaxel. As shown in Figure 6A, microtubules detached in a similar manner in wild-type and HAβ5-overexpressing cells. Detached microtubules persisted for varying lengths of time, continued to grow and shorten from the plus end, but only displayed periods of pause or shortening from the minus end as has been reported before (Keating *et al.*, 1997; Ganguly *et al.*, 2010; Yang *et al.*, 2010). In agreement with previous studies (Ganguly *et al.*, 2010; Yang *et al.*, 2010), we found no evidence for fragment formation by microtubule nucleation away from the centrosome and found only very rare instances of lateral microtubule breaks. Moreover, neither of these events increased in frequency with HAβ5 overexpression.

The frequency of microtubule detachment was low in untreated wild-type cells but increased more than 10-fold in the HAβ5-expressing cells (Figure 6B). Low concentrations of paclitaxel that were able to suppress microtubule dynamics (Table S1) had no effect on microtubule detachment (Figure 6B). Although the very high density of microtubules around the centrosome made it difficult to

quantify microtubule detachment in HAβ5-expressing cells treated with even higher concentrations of paclitaxel or in wild-type cells depleted of β5-tubulin, we concluded that both treatments reduced microtubule detachment to near zero because we failed to see any such detachments in five separate cells observed for 5 min each and because we did not find any significant number of microtubule fragments that normally result from detachment events in hundreds of cells examined by immunofluorescence.

To test whether alterations in microtubule detachment or dynamics play the more critical role in affecting the ability of cells to divide, the percentage of cells that were large and multinucleated (a measure of whether they had problems in cell division) and the percentage of cells with at least five microtubule fragments (a measure of elevated rates of microtubule detachment) were plotted at a series of paclitaxel concentrations. The results showed that multinucleation of HAβ5-expressing cells was

prevented at the same relatively high drug concentrations that prevented microtubule fragments from forming (Figure 7). In contrast, the ability of paclitaxel to reduce the microtubule shortening rate occurred at much lower drug concentrations that did not restore normal cell division. We conclude that the ability of elevated β5 to inhibit cell division is principally caused by its ability to stimulate microtubule detachment from centrosomes and that paclitaxel is able to reverse this effect at the same concentrations that rescue cell division.

### DISCUSSION

Vertebrate β-tubulins can be sorted into two groups based on their protein sequence homology (Sullivan, 1988). Members of one group (β1, β2, β4a, and β4b) are highly conserved and differ by only 8–11 amino acids outside of their hypervariable C-terminal tails. Members of the second group (β3, β5, and β6) are much less well

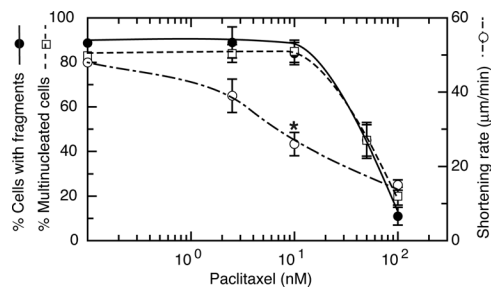


**FIGURE 7:** Abnormal cell division correlates with the presence of microtubule fragments. HAβ5ptx cells were grown for 2 d in the absence and presence of increasing concentrations of paclitaxel. The cells were then fixed and stained with anti-HA antibodies and DAPI. The percentage of multinucleated cells (open squares) and the percentage of cells with more than five microtubule fragments (closed circles) were plotted against the paclitaxel concentration. Also plotted are the microtubule shortening rates (open circles) at each drug concentration (see Supplemental Table S1). Note that the shortening rate at 10 nM paclitaxel (marked with an asterisk) is similar to the shortening rate for untreated wild-type cells (see Supplemental Table S1), yet multinucleation is unchanged.

conserved and differ at 21–85 residues outside of their C-terminal tails. By overexpressing each individual isotype in CHO cells under the control of an inducible promoter, we previously showed that  $\beta 1$ ,  $\beta 2$ , or  $\beta 4b$  had no effect on cell proliferation, microtubule assembly, or cell sensitivity to paclitaxel (Blade *et al.*, 1999). With  $\beta 4a$  overexpression, only subtle effects were seen: low expression sensitized the cells to paclitaxel because of a presumed increase in drug binding affinity, but the increased sensitivity was lost at higher expression because of weak paclitaxel resistance induced by weak inhibition of microtubule assembly (Yang and Cabral, 2007). Overexpression of  $\beta 3$ , a neuronal and testis-specific tubulin isotype (Luduena, 1998), produced a somewhat larger effect: moderate expression reduced microtubule assembly and conferred weak paclitaxel resistance, whereas high expression caused a greater disruption of the microtubules and made the cells dependent on paclitaxel for cell division (Hari *et al.*, 2003). The largest effects reported to date, however, were associated with  $\beta 5$ . Even relatively low overexpression of this isotype inhibited microtubule assembly and conferred paclitaxel resistance; moderate expression strongly disrupted the microtubule cytoskeleton, left behind only a few long microtubules as well as many smaller fragments, and conferred paclitaxel dependence (Bhattacharya and Cabral, 2004). Despite the toxicity caused by  $\beta 5$  overexpression, it is an isotype that is expressed in most tissues at low levels (Sullivan *et al.*, 1986) and it is essential for cell division in CHO and other cultured cell lines (Bhattacharya *et al.*, 2008).

In an effort to understand the basis for  $\beta 5$ 's ability to disrupt microtubule assembly, we overexpressed  $\beta 5$  and found that it doubled the rate of shortening. We envisage a simple mechanism to explain this. CHO cell microtubules are composed of 70%  $\beta 1$ , 25%  $\beta 4b$ , and 5%  $\beta 5$  (Ahmad *et al.*, 1991; Sawada and Cabral, 1989). Because  $\beta 1$  and  $\beta 4b$  differ at only eight internal residues (i.e., exclusive of the C-terminal tail), microtubules constructed with only these two subunits would be expected to have a good "fit," that is, longitudinal and lateral interactions would be maximized. The introduction of  $\beta 5$  subunits, which differ from  $\beta 1$  and  $\beta 4b$  at roughly 30 internal residues, would weaken the microtubule lattice by introducing areas of imperfect fit. At low stoichiometry (e.g., 5% in CHO cells), these imperfections would make the microtubules less stable and better able to remodel; but when present at too high a level, would cause microtubule disruption (Bhattacharya and Cabral, 2004) by facilitating the loss of subunits.

This model is supported by our observations on the presence of "GTP remnants." These remnants represent regions of the microtubule that retain  $\beta$ -tubulin in an assembly-competent conformation and have been suggested to act as sites where rescue, the transition of shortening microtubules to a growth or pause phase, can occur (Dimitrov *et al.*, 2008). Our data support this interpretation: increased  $\beta 5$  diminishes these remnants and produces long uninterrupted microtubule shortening events, whereas  $\beta 5$  depletion increases GTP remnants and produces microtubules that exhibit only very brief episodes of depolymerization.

Exactly how  $\beta 5$  controls the existence of GTP remnants is not clear. It is unlikely that  $\beta 5$  is depleted in GTP remnants relative to the remainder of the microtubule because numerous immunofluorescence studies of cell lines with either low or high expression of  $\beta 5$  have failed to show any noncontinuous distribution of this isotype along the microtubule lattice. Given that the antibody recognizes the conformation rather than the nucleotide-bound state of  $\beta$ -tubulin, the GTP remnants could represent tubulin subunits that actually retain GTP (implying that  $\beta 5$  facilitates GTP hydrolysis) or they could more simply be composed of tubulin that is locked into its "straight" assembly-favorable conformation by subunit-subunit

interactions within the microtubule lattice or by other unknown mechanisms. We propose that GTP remnants may be dynamic regions that disappear when the lattice is stressed in such a way as to weaken subunit interactions, but reform in a cooperative manner when a critical number of subunit interactions force tubulin into its straight conformation. The incorporation of  $\beta 5$  might loosen the interactions within the lattice, thereby increasing the frequency at which tubulin relaxes into its "curved" assembly-unfavorable conformation and making it more difficult to establish areas with tubulin in the straight conformation. Together, these changes would serve to limit the number and size of GTP remnants.

In other studies, we reported that the effects of  $\beta 5$  on microtubule stability could be traced to a single S239 residue (Bhattacharya and Cabral, 2009). This residue is a cysteine in isotypes  $\beta 1$  and  $\beta 4b$  that make up 95% of the  $\beta$ -tubulin in CHO cells. C239 is very close to C354 when group 1 isotypes are in their assembly-competent "straight" conformation, and we previously speculated that their interaction might be involved in maintaining this conformation (Bhattacharya and Cabral, 2009). By this reasoning, the 5%  $\beta 5$ -tubulin normally present in CHO cells could be introducing instability into the microtubule lattice because it is unable to form the C239/C354 interaction. This would explain the increase in GTP remnants and the hyperstabilization of microtubules that we saw in  $\beta 5$ -depleted cells. It would also explain the loss of GTP remnants, and the increased depolymerization rates and distances, when HA $\beta 5$  was incorporated in high abundance into the microtubule lattice.

Despite the potent effects of  $\beta 5$  on microtubule dynamics, those changes are insufficient to explain the ability of  $\beta 5$  to disrupt microtubules because 10 nM paclitaxel largely reversed the effects on dynamic instability as well as the rapid and uninterrupted shortening of microtubules in HA $\beta 5$ -overexpressing cells, but it did not eliminate microtubule fragments or allow cell division. A 10-fold-higher (100 nM) concentration of paclitaxel was needed to reverse these latter defects, indicating that fragments produced by microtubule detachment from centrosomes play an essential role in the mechanism by which  $\beta 5$ -tubulin disrupts the microtubule cytoskeleton. Microtubule detachment has also been implicated in the ability of mutant  $\beta 1$ -tubulins to confer paclitaxel resistance and dependence (Ganguly *et al.*, 2010) and in the action of microtubule disruptive drugs that inhibit cell division (Yang *et al.*, 2010). It appears to be a natural but low-frequency process that was previously observed in PtK1 and L929 cells (Keating *et al.*, 1997; Abal *et al.*, 2002).

The mechanism responsible for microtubule detachment is unknown. One possibility is that microtubules are occasionally pulled away from the centrosome by mechanical stress or other forces. We do not currently favor this possibility because we have thus far found no evidence for the presence of centrosomal proteins at the minus ends of detached microtubules, and because the rate of microtubule detachment rises at prophase, suggesting that it is a regulated process required for spindle formation and cell division (Yang *et al.*, 2010). Instead, we favor the idea that microtubule detachment requires the action of centrosomal proteins that become activated upon entry into mitosis. The observation that increased microtubule detachment is induced by drugs (Yang *et al.*, 2010), changes in tubulin isotype composition (the studies described here), or diverse mutations in  $\beta 1$ -tubulin (Ganguly *et al.*, 2010) suggests that the process does not depend on specific enzyme/substrate recognition sequences. Rather, we speculate that destabilizing or severing proteins at the centrosome may be better able to disrupt microtubules that contain imperfections in the lattice introduced through multiple pathways.

The results of this study indicate that  $\beta 5$ -tubulin affects critical aspects of microtubule behavior. The small amount of  $\beta 5$ -tubulin in CHO and other cells may be needed to maintain microtubule plasticity as indicated by the observation that  $\beta 5$  depletion hyperstabilized microtubules and inhibited cell division (Bhattacharya *et al.*, 2008). On the other hand, too much  $\beta 5$  production, as seen in HA $\beta 5$ -overexpressing cells, made the microtubules too unstable and again inhibited cell division. It is of interest that nondividing neuronal cells lack  $\beta 5$  but express  $\beta 3$ , another group 2  $\beta$ -tubulin isotype that has the Ser-239 residue and is capable of disrupting microtubule assembly (Hari *et al.*, 2003). It is tempting to speculate that  $\beta 3$  may play a  $\beta 5$ -like function in neuronal cells, but if so, it is unlikely to be an exact replacement. We have found that  $\beta 3$  disrupts microtubule assembly much more weakly than  $\beta 5$  (Hari *et al.*, 2003), and our attempts to rescue  $\beta 5$ -depleted cells with  $\beta 3$  have been unsuccessful (Bhattacharya and Cabral, unpublished studies). These isotype replacement experiments are difficult and could have failed for technical reasons, but we favor the idea that  $\beta 3$  and  $\beta 5$  may have overlapping but nonidentical functions. We further suggest that tissues may use different tubulin isotype compositions to satisfy a need for different microtubule properties. Unlike regulation by microtubule-interacting proteins that may exert localized or transient effects on microtubule behavior, the expression of different tubulin isoforms with their long half-lives is better suited for the more permanent specification of microtubule assembly properties. Thus  $\beta 5$  may be needed for producing the more dynamic mitotic microtubules of dividing cells, whereas  $\beta 3$  may be more suited for the production of axonal microtubules in nondividing neuronal cells. The existence of  $\beta$ -tubulin isoforms that can modulate microtubule behavior and are either widely or narrowly expressed suggests that cells may be able to dictate microtubule properties by specifying the ratio of  $\beta$ -tubulin isoforms that they express.

## MATERIALS AND METHODS

### Plasmids and constructs

pTOP-HA $\beta 5$  (Bhattacharya and Cabral, 2004) expresses an HA-tagged mouse  $\beta 5$ -tubulin cDNA (GenBank Accession No. BC008225) under the control of a tetracycline-regulated promoter. Plasmid pBSU6-c $\beta 5$  that transcribes shRNA targeting CHO  $\beta 5$ -tubulin and pHygro/U6-c $\beta 5$ , a similar plasmid that additionally encodes a hygromycin-resistance gene, were previously described (Bhattacharya *et al.*, 2008). pmCherryH2B-c $\beta 5$ , which coexpresses mCherry-H2B and the  $\beta 5$ -shRNA, was constructed by excising the U6 promoter and shRNA template from pBSU6-c $\beta 5$  and inserting it into the plasmid pmCherryC3-H2B (kind gift from Wei Jiang, Burnham Institute). A plasmid that expresses EGFP-MAP4 (Olson *et al.*, 1995) came from Joanna Olmsted (University of Rochester) and a plasmid able to express EB1-GFP (Piehl and Cassimeris, 2003) was obtained through Addgene (Cambridge, MA).

### Transfected cell lines

HA $\beta 5$ c8, a stably transfected CHO cell line that expresses HA $\beta 5$ -tubulin under the control of a tetracycline-regulated promoter was previously described (Bhattacharya and Cabral, 2004). This cell line grows normally when HA $\beta 5$  expression is repressed by the presence of tetracycline but requires paclitaxel for proliferation when tetracycline is removed. To obtain cells able to divide normally while expressing HA $\beta 5$ -tubulin, HA $\beta 5$ c8 was maintained in 300 nM paclitaxel without tetracycline to obtain cell line HA $\beta 5$ ptx. The two cell lines had a similar high level of HA $\beta 5$  expression. To deplete  $\beta 5$ , wild-type CHO cells were transfected with pBSU6-c $\beta 5$  or pmCherryH2B-c $\beta 5$  using lipofectamine (Invitrogen, Carlsbad, CA) as

described before (Bhattacharya *et al.*, 2008). Most experiments were performed 4 d after transfection to allow for the depletion of preexisting  $\beta 5$ -tubulin. To measure acetylated tubulin in cells with reduced  $\beta 5$ -tubulin, CHO cells were transfected with pHygro/U6- $\beta 5$  and then selected in presence of 500  $\mu$ g/ml hygromycin for 6–7 d to kill untransfected cells and enrich for cells with low  $\beta 5$ -tubulin content. For live cell imaging experiments, cells were transfected with EGFP-MAP4, and microtubules were viewed 24–48 h later. For quantification of acetylated tubulin, Western blots were probed with antibodies to acetylated tubulin and to actin as described below.

### Immunostaining

Cells on glass coverslips were extracted with microtubule stabilizing buffer (20 mM Tris-HCl, pH 6.8, 1 mM MgCl<sub>2</sub>, 2 mM EGTA, 0.5% Nonidet P-40) containing 4  $\mu$ g/ml paclitaxel (Sigma-Aldrich, St. Louis, MO) for 2 min at 4°C. After fixation in methanol at –20°C for 15 min, the cells were rehydrated in phosphate-buffered saline (PBS) for 15 min and incubated in PBS containing 1:50 or 1:200 dilutions of primary antibodies for 1 h at 37°C in a humid chamber. The coverslips were then washed in PBS and incubated for 1 h in 1:50 dilutions of Alexa 488-conjugated goat anti-rabbit or Alexa 594-conjugated goat anti-mouse immunoglobulin (Ig)G (Invitrogen) containing 1  $\mu$ g/ml DAPI. After washing in PBS, the coverslips were inverted onto 10  $\mu$ l of Gel/Mount (BioMeda, Foster City, CA) and viewed by epifluorescence using an Optiphot microscope (Nikon, Melville, NY). Images were obtained with a MagnaFire color digital camera (Optronics, Goleta, CA). The antibodies used included mouse monoclonal DM1A (Sigma-Aldrich) against  $\alpha$ -tubulin, affinity purified rabbit antibodies prepared against the C-terminal peptide of rodent  $\beta 5$ -tubulin (gift of Anthony Frankfurter, University of Virginia), a rabbit polyclonal antibody against the HA-tag (Bethyl Labs, Montgomery, TX), mouse monoclonal antibody (mAb) 611B1 (Sigma-Aldrich) against acetylated  $\alpha$ -tubulin, rabbit polyclonal X2 against  $\alpha$ -tubulin (Gundersen *et al.*, 1984), mouse mAb C4 against actin (Millipore, Billerica, MA), humanized recombinant antibody hMB11 against the GTP-bound conformation of tubulin (Dimitrov *et al.*, 2008), and various secondary antibodies (Invitrogen).

For experiments using the tubulin conformation-sensitive antibody hMB11, we modified a previously described procedure (Dimitrov *et al.*, 2008). Cells attached to glass coverslips were pre-extracted 2 min in a low ionic strength PEMG<sub>low</sub> buffer (20 mM PIPES, pH 6.8, 2 mM MgCl<sub>2</sub>, 2 mM EGTA, and 10% glycerol) containing 0.1% Triton X-100. The coverslips were then inverted onto 10  $\mu$ l of higher ionic strength PEMG<sub>high</sub> buffer (100 mM PIPES, pH 6.8, 2 mM MgCl<sub>2</sub>, 2 mM EGTA, and 10% glycerol) containing 0.2% bovine serum albumin (BSA) and hMB11 (1:400 dilution) and incubated in a humid chamber at 37°C for 15–20 min. After washing gently in PEMG<sub>high</sub> buffer three times, the coverslips were incubated with Alexa 594-conjugated anti-human IgG (1:50 dilution) in PEMG<sub>high</sub> containing 0.2% BSA for 15 min, washed three times with PEMG<sub>high</sub>, and fixed at –20°C in methanol. Subsequent staining with other antibodies was carried out as described above for fixed cells.

### Live cell imaging

Cells on 22-mm circular glass coverslips were transiently transfected with EGFP-MAP4. At 24–48 h posttransfection, the coverslips were inverted onto indented glass slides (Fisher Scientific, Pittsburgh, PA) filled with McCoys 5A media containing 25 mM HEPES (Mediatech, Manassas, VA) and sealed using sterilized vacuum grease. Microtubules were visualized using the 100 $\times$  oil objective on a DeltaVision Core imaging system (Applied Precision, Issaquah, WA) maintained at 37°C. Images were obtained at 5-s intervals for 50 or 100 frames.



Changes in microtubule length with time were measured by opening an image stack in ImageJ (NIH, Bethesda, MD) and tracing individual microtubules in successive images from a fixed starting point using the line tool. Lengths were tabulated and graphed to obtain microtubule life history plots that could subsequently be used to calculate various parameters of dynamic instability. The minimum change in length that was recorded as a true growth or shrinkage event was 0.5  $\mu\text{m}$ , and only microtubules that persisted for at least 120 s were used in calculating the dynamic parameters.

### Nucleation assay

Cells grown on glass coverslips were incubated in media containing 150 ng/ml colcemid for 2 h to depolymerize interphase microtubules. The coverslips were then washed three times in PBS and incubated in fresh media at 37°C. At different time points, coverslips were taken out and processed for immunostaining. In an alternative assay, cells were transfected with EB1-GFP and imaged every 5 s using a DeltaVision microscope. Nucleation events were measured by opening a stack of images in ImageJ and counting newly formed EB1-GFP comets in subsequent frames that traversed an annulus defined by two concentric circles (3.5 and 7.5  $\mu\text{m}$  diameter) around the centrosome.

### Electrophoresis and Western blots

Proteins from cells growing in 24-well dishes were solubilized in 1% SDS, precipitated with 5 volumes of 4°C acetone, resuspended in sample buffer (0.0625 M Tris-HCl, pH 6.8, 2.5% SDS, 5% 2-mercaptoethanol, 10% glycerol), fractionated on a 7.5% polyacrylamide SDS minigel, and transferred to PROTRAN nitrocellulose membranes (Schleicher and Schuell, Keene, NH). The membranes were blocked by incubating 1 h in PBST (PBS with 0.05% Tween 20) with 3% dry milk. After washing in PBST three times, the membranes were incubated 1 h in acetylated  $\alpha$ -tubulin-specific antibody 611B1 (1:2000 dilution in PBST + 0.2% BSA) and actin-specific antibody C4 (1:25000 dilution) to act as a gel-loading control. Following three washes in PBST, the blots were incubated 1 h in Alexa 647-conjugated goat anti-mouse IgG (1:2000 dilution) and washed in PBS. Reacting protein bands were detected by capturing fluorescence emission on a STORM 860 imager (Molecular Dynamics, Sunnyvale, CA). Relative levels of acetylated tubulin among different cell lines were determined by comparing their ratios of acetylated  $\alpha$ -tubulin to actin. Mouse mAb 18D6 against the highly conserved N terminus of  $\beta$ -tubulin (1:5000 dilution) (Theodorakis and Cleveland, 1992) or the polyclonal antibody against the rodent  $\beta$ 5-tubulin (1:10,000 dilution) were used to detect levels of total  $\beta$ -tubulin or  $\beta$ 5-tubulin, respectively.

### ACKNOWLEDGMENTS

We thank Joanna Olmsted, University of Rochester, for the EGFP-MAP4 plasmid; Wei Jiang, The Burnham Institute, for the pmCherryC3-H2B plasmid; Franck Perez, Institut Curie, for the hMB11 antibody; Anthony Frankfurter, University of Virginia, for the  $\beta$ 5-tubulin-specific antibody; Jeannette Bulinski, Columbia University, for antibody X2 against  $\alpha$ -tubulin; and Don Cleveland, Ludwig Institute for Cancer Research, for antibody 18D6. We are indebted to Xiangwei He, Baylor College of Medicine, for generously allowing us to use his DeltaVision microscope. These studies were supported by grants (to F.C.) from the National Science Foundation and the National Institutes of Health.

### REFERENCES

Abal M, Piel M, Bouckson-Castaing V, Mogensen M, Sibarita JB, Bornens M (2002). Microtubule release from the centrosome in migrating cells. *J Cell Biol* 159, 731–737.

Abraham I, Marcus M, Cabral F, Gottesman MM (1983). Mutations in  $\alpha$ - and  $\beta$ -tubulin affect spindle formation in Chinese hamster ovary cells. *J Cell Biol* 97, 1055–1061.

Ahmad S, Singh B, Gupta RS (1991). Nucleotide sequences of three different isoforms of beta-tubulin cDNA from Chinese hamster ovary cells. *Biochim Biophys Acta* 1090, 252–254.

Akhmanova A, Steinmetz MO (2008). Tracking the ends: a dynamic protein network controls the fate of microtubule tips. *Nat Rev Mol Cell Biol* 9, 309–322.

Banerjee A, Luduena RF (1992). Kinetics of colchicine binding to purified beta-tubulin isotypes from bovine brain. *J Biol Chem* 267, 13335–13339.

Barlow SB, Gonzalez-Garay ML, West RR, Olmsted JB, Cabral F (1994). Stable expression of heterologous microtubule associated proteins in Chinese hamster ovary cells: evidence for differing roles of MAPs in microtubule organization. *J Cell Biol* 126, 1017–1029.

Bhattacharya R, Cabral F (2004). A ubiquitous  $\beta$ -tubulin disrupts microtubule assembly and inhibits cell proliferation. *Mol Biol Cell* 15, 3123–3131.

Bhattacharya R, Cabral F (2009). Molecular basis for class V  $\beta$ -tubulin effects on microtubule assembly and paclitaxel resistance. *J Biol Chem* 284, 13023–13032.

Bhattacharya R, Frankfurter A, Cabral F (2008). A minor  $\beta$ -tubulin essential for mammalian cell proliferation. *Cell Motil Cytoskeleton* 65, 708–720.

Blade K, Menick DR, Cabral F (1999). Overexpression of class I, II, or IV  $\beta$ -tubulin isotypes in CHO cells is insufficient to confer resistance to paclitaxel. *J Cell Sci* 112, 2213–2221.

Bond JF, Fridovich-Keil JL, Pillus L, Mulligan RC, Solomon F (1986). A chicken-yeast chimeric  $\beta$ -tubulin protein is incorporated into mouse microtubules in vivo. *Cell* 44, 461–468.

Cabral F, Barlow SB (1991). Resistance to antimetabolic agents as genetic probes of microtubule structure and function. *Pharmac Ther* 52, 159–171.

Dimitrov A, Quesnoit M, Moutel S, Cantaloube I, Pous C, Perez F (2008). Detection of GTP-tubulin conformation in vivo reveals a role for GTP remnants in microtubule rescues. *Science* 322, 1353–1356.

Fulton C, Simpson PA (1976). Selective synthesis and utilization of flagellar tubulin. The multi-tubulin hypothesis. In: *Cell Motility*, eds. R Goldman, T Pollard, and J Rosenbaum, New York: Cold Spring Harbor Press, 987–1006.

Ganguly A, Yang H, Cabral F (2010). Paclitaxel dependent cell lines reveal a novel drug activity. *Mol Cancer Ther* 9, 2914–2923.

Gundersen GG, Kalnoski MH, Bulinski JC (1984). Distinct populations of microtubules: tyrosinated and nontyrosinated alpha tubulin are distributed differently in vivo. *Cell* 38, 779–789.

Hari M, Yang H, Zeng C, Canizales M, Cabral F (2003). Expression of class III  $\beta$ -tubulin reduces microtubule assembly and confers resistance to paclitaxel. *Cell Motil Cytoskeleton* 56, 45–56.

Hoyle HD, Raff EC (1990). Two *Drosophila* beta tubulin isoforms are not functionally equivalent. *J Cell Biol* 111, 1009–1026.

Jordan MA, Toso RJ, Thrower D, Wilson L (1993). Mechanism of mitotic block and inhibition of cell proliferation by taxol at low concentrations. *Proc Natl Acad Sci USA* 90, 9552–9556.

Jordan MA, Wilson L (1998). Use of drugs to study role of microtubule assembly dynamics in living cells. *Methods Enzymol* 298, 252–276.

Jordan MA, Wilson L (2004). Microtubules as a target for anticancer drugs. *Nat Rev* 4, 253–265.

Joshi HC, Yen TJ, Cleveland DW (1987). In vivo coassembly of a divergent  $\beta$ -tubulin subunit ( $\beta$ 6) into microtubules of different function. *J Cell Biol* 105, 2179–2190.

Kamath K, Wilson L, Cabral F, Jordan MA (2005).  $\beta$ III-tubulin induces paclitaxel resistance in association with reduced effects on microtubule dynamic instability. *J Biol Chem* 280, 12902–12907.

Keating TJ, Peloquin JG, Rodionov VI, Momcilovic D, Borisy GG (1997). Microtubule release from the centrosome. *Proc Natl Acad Sci USA* 94, 5078–5083.

Kung AL, Sherwood SW, Schimke RT (1990). Cell line-specific differences in the control of cell cycle progression in the absence of mitosis. *Proc Natl Acad Sci USA* 87, 9553–9557.

Lewis SA, Gu W, Cowan NJ (1987). Free intermingling of mammalian  $\beta$ -tubulin isotypes among functionally distinct microtubules. *Cell* 49, 539–548.

Lopata MA, Cleveland DW (1987). In vivo microtubules are copolymers of available  $\beta$ -tubulin isotypes: localization of each of six vertebrate  $\beta$ -tubulin isotypes using polyclonal antibodies elicited by synthetic peptide antigens. *J Cell Biol* 105, 1707–1720.

Lu Q, Luduena RF (1994). In vitro analysis of microtubule assembly of isotypically pure tubulin dimers. *J Biol Chem* 269, 2041–2047.

- Ludueno RF (1998). Multiple forms of tubulin: different gene products and covalent modifications. *Int Rev Cytol* 178, 207–275.
- Maruta H, Greer K, Rosenbaum JL (1986). The acetylation of  $\alpha$ -tubulin and its relationship to the assembly and disassembly of microtubules. *J Cell Biol* 103, 571–579.
- May GS (1989). The highly divergent  $\beta$ -tubulins of *Aspergillus nidulans* are functionally interchangeable. *J Cell Biol* 109, 2267–2274.
- Mitchison T, Kirschner MW (1984). Dynamic instability of microtubules. *Nature* 312, 237–242.
- Mitchison TJ, Kirschner MW (1987). Some thoughts on the partitioning of tubulin between monomer and polymer under conditions of dynamic instability. *Cell Biophys* 11, 35–55.
- Olson KR, McIntosh JR, Olmsted JB (1995). Analysis of MAP 4 function in living cells using green fluorescent protein (GFP) chimeras. *J Cell Biol* 130, 639–650.
- Panda D, Miller HP, Banerjee A, Ludueno RF, Wilson L (1994). Microtubule dynamics in vitro are regulated by the tubulin isotype composition. *Proc Natl Acad Sci USA* 91, 11358–11362.
- Piehl M, Cassimeris L (2003). Organization and dynamics of growing microtubule plus ends during early mitosis. *Mol Biol Cell* 14, 916–925.
- Savage C, Hamelin M, Culotti JG, Coulson A, Albertson DG, Chalfie M (1989). *mec-7* is a  $\beta$ -tubulin gene required for the production of 15-protofilament microtubules in *Caenorhabditis elegans*. *Genes Dev* 3, 870–881.
- Sawada T, Cabral F (1989). Expression and function of  $\beta$ -tubulin isotypes in Chinese hamster ovary cells. *J Biol Chem* 264, 3013–3020.
- Schwer HD, Lecine P, Tiwari S, Italiano JEJ, Hartwig JH, Shivdasani RA (2001). A lineage-restricted and divergent  $\beta$ -tubulin isoform is essential for the biogenesis, structure and function of blood platelets. *Curr Biol* 11, 579–586.
- Sullivan KF (1988). Structure and utilization of tubulin isotypes. *Annu Rev Cell Biol* 4, 687–716.
- Sullivan KF, Havercroft JC, Machlin PS, Cleveland DW (1986). Sequence and expression of the chicken  $\beta$ 5- and  $\beta$ 4-tubulin genes define a pair of divergent  $\beta$ -tubulins with complementary patterns of expression. *Mol Cell Biol* 6, 4409–4418.
- Takahashi M, Shiraishi H, Ishibashi Y, Blade KL, McDermott PJ, Menick DR, Kuppuswamy D, Cooper G (2003). Phenotypic consequences of  $\beta$ 1-tubulin expression and MAP4 decoration of microtubules in adult cardiocytes. *Am J Physiol Heart Circ Physiol* 285, H2072–H2083.
- Theodorakis NG, Cleveland DW (1992). Physical evidence for cotranslational regulation of  $\beta$ -tubulin mRNA degradation. *Mol Cell Biol* 12, 791–799.
- Wang XM, Peloquin JG, Zhai Y, Bulinski JC, Borisy GG (1996). Removal of MAP4 from microtubules in vivo produces no observable phenotype at the cellular level. *J Cell Biol* 132, 345–357.
- Yang H, Cabral F (2007). Heightened sensitivity to paclitaxel in class IVa  $\beta$ -tubulin transfected cells is lost as expression increases. *J Biol Chem* 282, 27058–27066.
- Yang H, Ganguly A, Cabral F (2010). Inhibition of cell migration and cell division correlates with distinct effects of microtubule inhibiting drugs. *J Biol Chem* 285, 32242–32250.